Original Article

DOI: 10.5582/bst.2021.01245

# Soluble β-amyloid impaired the GABA inhibition by mediating KCC2 in early APP/PS1 mice

**Yuan Zhou[1,§], Yujie Cheng[1,§], Yong Li[1,§], Jiyao Ma[3], Zhihan Wu[3], Yuenan Chen[1], Jinyu Mei[2,*], Ming Chen[1,*]**

[1] Department of Pharmacology, School of Basic Medical Sciences, Anhui Medical University, Hefei, Anhui, China;
[2] Department of Otorhinolaryngology, Head and Neck Surgery, the Second Hospital of Anhui Medical University, Hefei, Anhui, China;
[3] First Clinical Medical College, Anhui Medical University, Hefei, Anhui, China.

**SUMMARY** Alzheimer's disease (AD) is a neurodegenerative disorder, which has become the leading cause of dementia cases globally. Synaptic failure is an early pathological feature of AD. However, the cause of synaptic failure in AD, especially the GABAergic synaptic activity remains unclear. Extensive evidence indicates that the presence of soluble amyloid-β is an early pathological feature in AD, which triggers synaptic dysfunction and cognitive decline. Our recent study explored the relation of GABAergic transmission and soluble Aβ in early APP/PS1 mice. Firstly, we found soluble Aβ42 levels were significantly increased in serum, hippocampus and prefrontal cortex in 3-4 months APP/PS1 mice, which was much earlier than Aβ plagues formation. In addition, we found TNF-α and BDNF expression levels were increased, while KCC2 and $GABA_AR$ expression were decreased in 3-4 months APP/PS1 hippocampus. When we treated 3-4 months APP/PS1 mice with a potent γ-secretase inhibitor, LY411575, which can reduce the soluble Aβ42 levels, the TNF-α and BDNF protein levels were decreased, while KCC2 and $GABA_AR$ levels were increased. In conclusion, our study suggested soluble Aβ may impaired the GABA inhibition by mediating KCC2 levels in early APP/PS1 mice. KCC2 may be served as a potential biomarker for AD.

***Keywords*** Alzheimer's disease, soluble β-amyloid, TNF-α, BDNF, KCC2, $GABA_AR$

## 1. Introduction

Alzheimer's disease (AD) is a neurodegenerative disorder, which characterized by progressive memory and cognitive impairment, and as the disease advances, symptoms include the loss of memory and motor skills, disorientation, failure to perform self-care, and finally the loss of bodily functions, which leads to the death (*1,2*). Although the cause of AD isn't completely understood, two major players that are often cited in its progression are plaques and tangles (*3*). Amyloid pathogenesis starts with altered cleavage of amyloid precursor protein (APP), an integral protein on the plasma membrane, by β-secretases (BACE1) and γ-secretases to produce insoluble Aβ fibrils, and Aβ then oligomerizes, diffuses into synaptic clefts, and interferes with synaptic signaling (*4,5*).

Microglial cells can clear soluble and fibrillar Aβ, however, continued interactions of these cells with Aβ can lead to an inflammatory response resulting in neurotoxicity (*6*). Aβ oligomers and fibrils are capable of priming microglial cells through interactions with various receptors, which enhance the production of inflammatory cytokines and chemokines (interleukin-1 (IL-1), interleukin-6 (IL-6), interleukin-8 (IL-8) and tumor necrosis factor α (TNF-α), C1q, *etc.*) and make microglia more susceptible to secondary stimuli, promoting microglial activation (*7,8*). Numerous studies indicated that TNF-α levels are higher in the cerebrospinal fluid (CSF) of AD patients compared to cognitively normal controls (*9-11*). Aβ can induce the release of high levels of TNF-α from primary cultures of rodent and human microglial cells (*9*). High levels of TNF-α increase the production of other pro-inflammatory cytokines, such as IL-1, IL-6, and IL-8, that can participate in the development of chronic neuroinflammation (*9,10*). TNF-α overproduction has also been associated with lower hippocampal volume and with a greater likelihood of mild cognitive impairment (MCI) patient conversion to AD (*12-14*). TNF-α, a pivotal role in neuroinflammation, is a very attractive pharmacological target, which used to reduce TNF-α signaling in rodent models of AD showed a significant reduction in AD-like brain pathology accompanied by an

amelioration of cognitive function (*9,12*).

Brain-derived neurotrophic factor (BDNF), an neurotrophins, can promote nervous system development, maintain neuronal plasticity and repair damaged neurons, but its excess can cause the opposite effect (*15,16*). TNF-α can up-regulate the expression of exon-IV-BDNF mRNA and BDNF protein in nerve injury tissues and astrocytes (*17-19*). BDNF-induced TrkB inhibited $GABA_A$ synaptic responses by down-regulates the expression of $K^+$-$Cl^-$ cotransporter KCC2 and impairs neuronal $Cl^-$ extrusion (*15,20-22*). The BDNF that secreted from activated microglias and peri-lesion damaged neurons act on damaged neuron and inhibiting KCC2 mRNA transcription by the BDNF-TrkB pathway (*15*).

In the vertebrate brain, $GABA_A$ receptors mediate the majority of fast inhibition in the brain, which depends on the intracellular $Cl^-$ ($[Cl^-]_i$) concentration (*22,23*). KCC2, a $K^+$-$Cl^-$ cotransporter, is a neuronal isoform that is broadly expressed in the adult. KCC2 functions in setting the proper $[Cl^-]_i$ by transporting $Cl^-$ against the concentration gradient (*24*). Thus, KCC2 is a crucial regulator of GABA-mediated hyperpolarization. Loss of KCC2 activity orchestrates a depolarizing shift in $E_{GABA}$ and is implicated in cortical development systems such as neuro- and synaptogenesis (*25,26*). The treatment of memantine, a drug that is currently prescribed for the treatment of AD, reduces the expression of KCC2 in the hippocampus and cerebral cortex and attenuates behavioral responses mediated by $GABA_AR$ activation in mice (*27*). There is a close linkage between the GABAergic signaling system and various aspect of AD pathology including Aβ toxicity (*28*), tau hyperphosphorylation and ApoE4 effect (*29*), which suggests that GABAergic system might undergo dynamic remodeling and play important roles in AD pathology.

Here, we found an increased soluble Aβ levels in 3-4 months APP/PS1 mice, which will lead to impaired GABA inhibition by mediating BDNF-TrkB-KCC2 pathway. When treated with γ-secretase inhibitors, these phenotypes can be rescued. The results indicate that KCC2 or $GABA_AR$ levels for the early diagnosis of AD.

## 2. Materials and Methods

### 2.1. Animals

All experimental procedures involving animals were performed in accordance with the guidelines for the humane treatment of animals by the Association of Laboratory Animal Sciences and were approved by the Center for Laboratory Animal Sciences at the Anhui Medical University. Every attempt was made to limit animal numbers and suffering. APP/PS1 double-transgenic mice were generated by crossing APP/PS1 and WT mice obtained from the Model Animal Research Center of Nanjing University (Nanjing, China). All mice were group kept in a clean laminar flow cabinet under SPF conditions at the Experimental Animal Center of Anhui Medical University (Anhui, China). The mice were housed in conventional cages at 20-25°C under a 12 h light/dark cycle, supplied with standard laboratory chow and water ad libitum. The mice were maintained under these conditions for at least 1 week for acclimatization before the commencement of experiments. All animals involved in experiments were 3-4 month-old unless otherwise indicated. At a certain age, mice were separately anesthetized. Brains were carefully dissected. Blood was collected. Brain tissues were preserved in 4% buffered paraformaldehyde solution at 4°C before the tissues were sliced at 4μm thickness (CRYOSTAR NX50, Thermo). Blood samples were centrifuged at 3500 rpm for 10 min (Hettich, Mikro 200R). Plasma was stored at -80°C until the ELISA was run.

### 2.2. Antibodies and reagents

KCC2 (Millipore, 07-432), $GABA_AR$ (Abcam, ab94585), $GABA_BR$ (Affinity, AF0162), BDNF (Affinity, DF6387), β-Amyloid 1-42 (Abcam, ab201060), TNF-α(Affinity, AF7014), IL-6 (Servicebio, GB11117), IL-1β (Affinity, AF5103), NLRP1 (Abcam, ab3683), NLRP3 (Abcam, ab214185), AMPAR (Abcam, ab31232), PSD95 (Thermo, MA1-045), Iba-1 (Servicebio, GB11105), GFAP (Servicebio, GB12096), β-Tubulin (Affinity, T0023), β-Actin (Affinity, AF7018), Goat Anti-Rabbit IgG (H+L) HRP (Affinity, S0001), Goat Goat Anti-Mouse IgG (H+L) HRP (Affinity, S0002).

### 2.3. Behavioral test

*Open fields test (OFT)* The open field test, also known as the open box test, is a commonly used animal behavior experiment. It is used to observe the spontaneous exploration of motor activity and anxiety behavior in mice. It is also a way to evaluate experimental animals' autonomous exploration of behavior and emotional tension in a new environment. The OFT instrument consists of two parts: an open field box (96 × 96 × 50 cm) and an automatic data acquisition system, the bottom of the open field box is equally divided into 9 squares. Install a camera about 2 meters directly above to record the experimental process in real time. First, place the mouse in the central area and let it crawl freely for 2 minutes to adapt to the environment. Then, record his total movement distance in 3 minutes, the number of times of threading, the time spent in the middle area and the distance moved. Before each test, clean the bottom of the open field box with ethanol to eliminate odor cues, and keep the room quiet.

*Elevated-plus maze (EPM)* High plus maze can be used to assess the anxiety level of animals. The height of the instrument is about 60 cm from the ground. It

consists of a set of open arms (30 × 5 cm) and a set of closed arms (30 × 5 × 15 cm) to cross vertically, and a central area (5 × 5 cm). Install a camera about 2 meters directly above to record the experimental process in real time. First, place the mouse in the central area facing the open arm, and let him explore freely for 5 minutes. The instrument will automatically record data, calculate the time and number of times the mouse enters the open arm. Before each test, clean the bottom of the open and closed arms with ethanol to eliminate odor cues and keep the room quiet.

*Forced swim test (FST)* Forced swim test (FST) is a behavioral test used to assess depression in mice. The mice are individually placed in a transparent plastic cylinder (height 50cm, 20cm in diameter, water depth 35cm, maintained at 25 ± 1℃) . Install a camera about 0.5 meters above to record in real time. Place the mouse in the water for 2 minutes, test the movement status of mice within 4 minutes, during the experiment, the mice will show three behaviors: struggling, swimming and standing still. Count the time the mice stayed still in the water during the experiment.

*Tail suspension test (TST)* The tail suspension test is a method used to evaluate depression in mice. Fix the tail of the mouse to the suspension rod with tape, make it head down. The suspension rod is fixed on a horizontal rod about 40 cm above the ground, each mouse is separated by opaque cardboard, the mouse is not less than 15 cm away from the surrounding space. First acclimate the mouse for 2 minutes, then test the mouse's twisting and struggling within 3 minutes, record its immobile time.

### 2.4. Hippocampal neuron cultures and treatment

HT22 neuron was maintained with Dulbecco's modified Eagle's medium (DMEM; Hyclone; Logan, USA) supplemented with 10% fetal bovine serum (FBS; Sijiqing, Zhejiang Tianhang Biological Technology Co., LTD; Huzhou, China) in a humidified incubator with an atmosphere of 5% $CO_2$ at 37°C. These cells at logarithmic growth were collected, counted and seeded at a density of $1 \times 10^6$ cells/25 $cm^2$ culture flask cultured in DMEM supplemented with 10% FBS. When these cells reached 80-90% confluency, the medium was replaced using the serum-free medium for 24 h and DMSO, TNF-α (PEPROTECH, AF-315-01A) and CLP257 (Sigma, SML1368-5MG) was added for 2 h, total proteins were extracted for followed western blot analysis.

### 2.5. Western blot

Hippocampus and prefrontal cortex tissue were obtained and homogenized using a lysis buffer and protease inhibitor. After 1 min of homogenization, the cellular debris was removed by centrifugation at 14000 rpm for 10 min at 4°C and supernatant were collected for denaturation for 20 min at 75°C. The lysate was then centrifuged on SDS-PAGE (Bio-Rad) under denaturing conditions and transferred to polyvinylidene difluoride (PVDF) microporous membrane. Membranes were blocked for 30 min using 5% non-fat dry milk in TBS containing 0.5% Tween-20 (TBST) and then incubated with specific primary antibodies against Aβ42, TNF-α, IL-6, IL-1β, BDNF, KCC2, $GABA_AR$, $GABA_BR$, NLRP1, NLRP3, AMPAR, PSD95. Anti β-Tubulin or β-Actin antibodies were used as the loading control. Antibodies were diluted at 1:1,000 to 1:2,000 at use. The next day, after three washes with TBST, the membranes were incubated with the corresponding secondary antibody (Affinity, S002) at room temperature (RT) for 1 h using 3% milk in TBST followed by three additional washes with TBST. Bands were visualized using a Chemi Doc TMMP Imaging System (Bio-Rad, USA) and analyzed with Gel Pro Analysis software. For the presentation in figures, digitalized blot images were processed and cropped using Adobe Illustrator to show the interested protein signals.

### 2.6. Immunofluorescent staining

The brain sections were sliced, antigen retrieved and blocked. Incubation of primary antibodies (Aβ42, Iba-1, GFAP) were done in carrier (PBS with 1% serum and 0.2% BSA) at 4°C overnight. After three washes with PBS, the sections were incubated in Rhodamine (TRITC)-Conjugated Goat anti-Rabbit IgG (ZSGB-BIO, ZF-0316) or FITC-Conjugated Goat anti-Mouse IgG (ZSGB-BIO, ZF-0312) at 37°C for 50 min. Washed with PBS, the sections were incubated in DAPI Staining Solution (Byotime, C1005) for 10 min. After three washes with PBS, the sections were mounted with Antifade Mounting Medium (Byotime, P0126-5ml), observed and photographed under a fluorescence microscope (Leica, Germany). The images were evaluated with ImageJ software (NIH, Bethesda, MD, USA).

### 2.7. Quantitative Real-time PCR (qRT-PCR)

Mice brains were dissected and immediately frozen in liquid nitrogen. Total RNA was extracted using Trizol reagent. RNA pellets were resuspended in diethylpyrocarbonate-treated water and RNA concentration was measured using a Nanodrop2000c spectrometer (Thermo Scientific). RNA was treated by the PrimeScript™ RT Master Mix (TaKaRa, Code No. RR036A) and then reverse-transcribed using the Bio-Rad T100TM thermal cycler. Relative quantification of gene expression was performed using the Bio-Rad CFX96™ Real-time System. Platinum Quantitative PCR P TB Green® Premix Ex Taq™ II (TaKaRa, Code No. RR820A) was used with the following primers and

probes:

TNF-α F-primer, 5'-CATGATCCGCGACGTGGAACTG-3';
TNF-α R-primer, 5'-AGAGGGAGGCCATTTGGGAACT-3';
BDNF F-primer, 5'-GGTATCCAAAGGCCAACTGA-3';
BDNF R-primer, 5'-CTTATGAATCGCCAGCCAAT-3';
Slc12a5 F-primer, 5'-GGGCAGAGAGTACGATGGC-3';
Slc12a5 R-primer, 5'-TGGGGTAGGTTGGTGTAGTTG-3';
β-Actin F-primer, 5'-GTGACGTTGACATCCGTAAAGA-3';
β-Actin R-primer, 5'- GTAACAGTCCGCCTAGAAGCAC-3';

Assay efficiencies were experimentally determined using a five-point dilution series of cDNA spanning a 100-fold range in concentration. 0.025 mg cDNA template was used per reaction. Statistical analysis was performed on $2^{-\Delta\Delta Cq}$ values.

2.8. Enzyme-linked immunosorbent assay (ELISA)

The supernatants of serum, hippocampus, and prefrontal cortex of WT and APP/PS1 mice were collected. The ELISA kit was used for the quantitative determination of Aβ42 (CUSABIO, CSB-E10787m), TNF-α (CUSABIO, CSB-E04741m), IL-6 (CUSABIO, CSB-E04639m), and IL-1β (CUSABIO, CSB-E08054m). Aβ42, TNF-α, IL-6, and IL-1β standards and samples were added to the wells of assay plates and incubated for 1 h at 37°C. Blank wells were added with standard diluent. The horseradish peroxidase (HRP) conjugated reagent (100 μL) was added to each well for 1 h at 37°C. Plates were washed four times with PBS, and chromogen solution (100 μL) was added to each well. The plates were gently mixed and incubated for 15 min at 37°C in the dark. Then, stop solution (50 μL) was added to each well and examined the absorbance at 450 nm with a microplate reader (SPECTRAMAX 190, USA) within 15 min.

2.9. Statistical analysis

Data were presented as mean ± standard error and analyzed using GraphPad Prism version 7.0 (GraphPad Software, La Jolla, CA, USA) by student's *t*-test or one-way ANOVA, as appropriate with $p < 0.05$ as statistically significant.

## 3. Results

3.1. Increased soluble Aβ42 in 3-4 months APP/PS1 mice

As shown in Figure 1, the ELISA result showed that the soluble Aβ42 were significantly increased in serum,

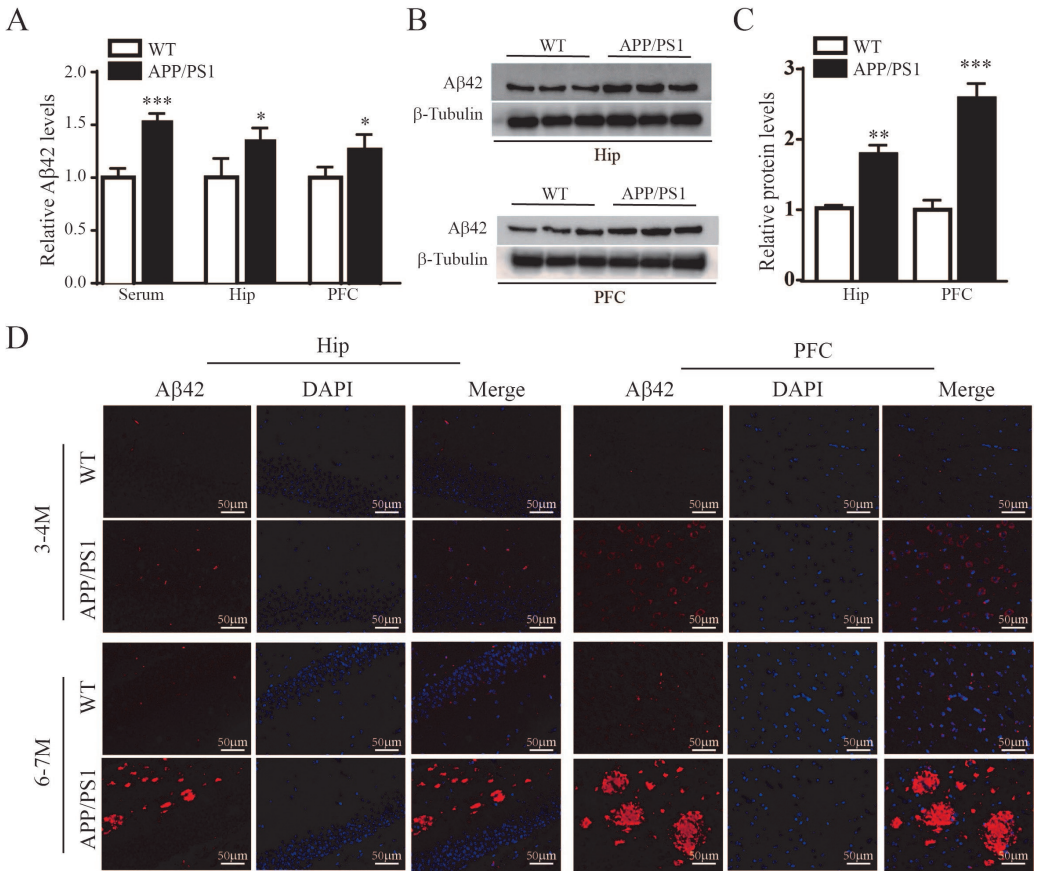


**Figure 1. Increased soluble Aβ42 level in 3-4 months APP/PS1 mice. (A)** The soluble Aβ42 levels in serum, hippocampus, and prefrontal cortex by ELISA. **(B)** Representative immunoblots of Aβ42 in the hippocampus and prefrontal cortex of WT and APP/PS1 mice. **(C)** Quantification of Aβ42 protein levels in (B). **(D)** Representative images of Aβ42 in the hippocampus and prefrontal cortex of 3-4 and 6-7 months WT and APP/PS1 mice. ($n = 6$ in each group, Student's *t*-test). All data are presented as mean ± SEM. $^{*}p < 0.05$, $^{**}p < 0.01$, $^{***}p < 0.001$.

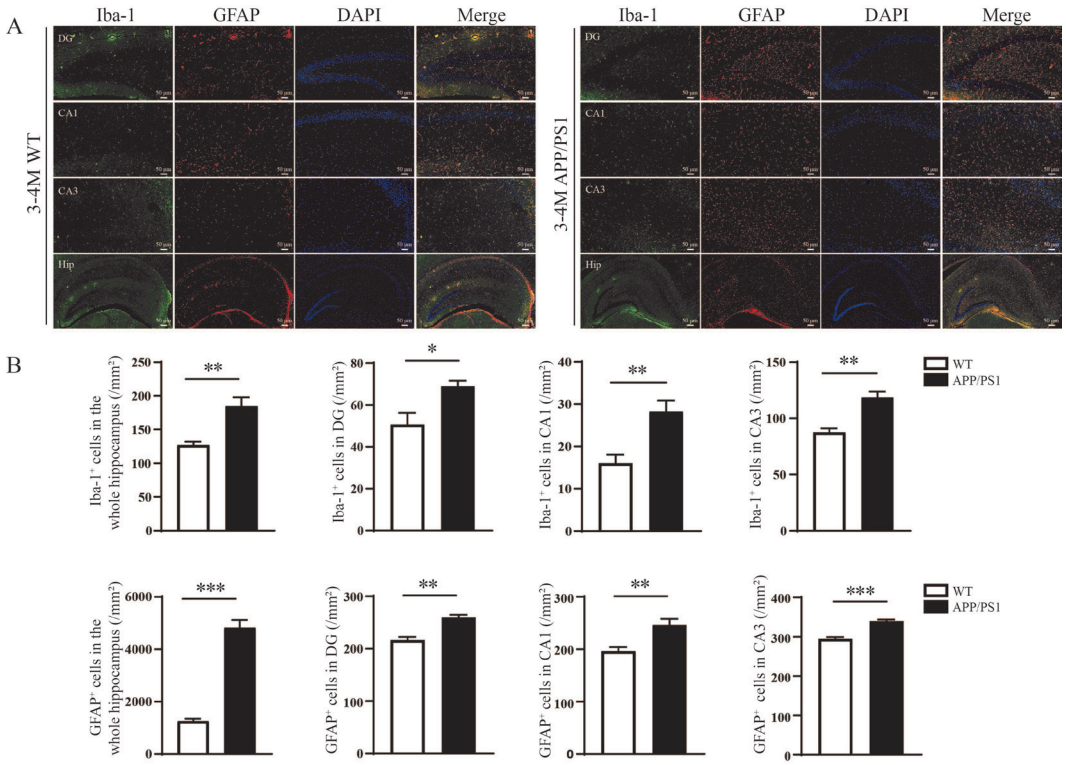


**Figure 2. APP/PS1 mice exhibit activated astrocyte and microglia in hippocampus. (A)** Representative images of Iba1+ and GFAP+ cells in 3-4 months APP/PS1 hippocampus. **(B)** Quantification of Iba1+ and GFAP+ cells in CA1, CA3, and DG of hippocampus in 3-4 months WT and APP/PS1 mice. ($n = 5$ in each group, Student's $t$-test). All data are presented as mean ± SEM. $^{*}p < 0.05$, $^{**}p < 0.01$, $^{***}p < 0.001$.

hippocampus and prefrontal cortex in 3-4 months APP/PS1 mice (Figure 1A). In addition, we also performed western blotting to detect Aβ42 protein levels in hippocampus and prefrontal cortex, and found that Aβ42 protein levels were significantly increased in 3-4 months APP/PS1 mice (Figure 1B-C). Immunofluorescent staining results showed more Aβ plaques in hippocampus and prefrontal cortex in 6-7 months APP/PS1 mice, but not in 3-4 months APP/PS1 mice (Figure 1D).

### 3.2. Activated glia cells and increased neuroinflammation in 3-4 months APP/PS1 mice

Aβ could cause neuroinflammation in the brain (*6*). In order to detect whether increased Aβ42 levels could induce neuroinflammation, we performed immunofluorescent staining to label glia cells. Compared with WT mice, the number of microglia and astrocytes were both increased significantly in 3-4 months APP/PS1 hippocampus (Figure 2A-B). To further test if increased soluble Aβ42 can lead to neuroinflammation, we detected TNF-α, IL-6 and IL-1β levels by ELISA kits and found these inflammatory factors were all increased in 3-4 months APP/PS1 mice (Figure 3A). Western blotting and real-time PCR results also showed an increased IL-1β and TNF-α protein and mRNA levels in hippocampus and prefrontal cortex of 3-4 months APP/PS1 (Figure 3B-E; Figure 6). NLRP1 and NLRP3 belong to NLR family and are both expressed in CNS (*30*). Activation of

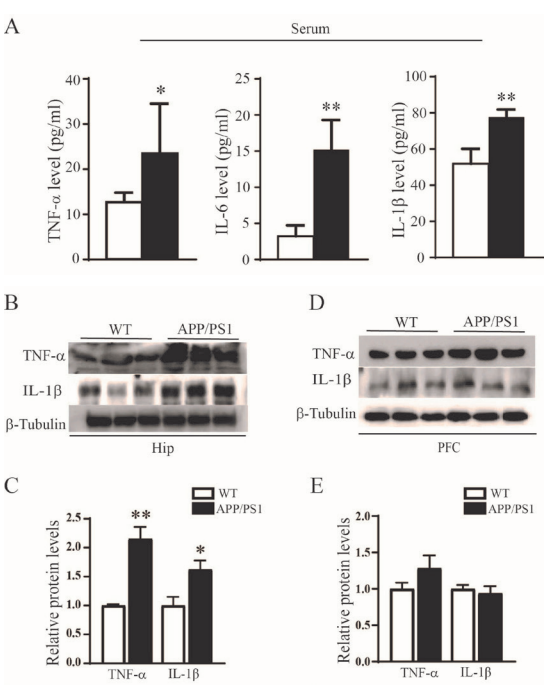


**Figure 3. Increased neuroinflammation in 3-4 months APP/PS1 hippocampus. (A)** TNF-α, IL-6, IL-1β levels in the serum of 3-4 months WT and APP/PS1 mice by ELISA. **(B)** Representative immunoblots of TNF-α and IL-1β in 3-4 months WT and APP/PS1 hippocampus. **(C)** Quantification of TNF-α and IL-1β protein levels in (B). **(D)** Representative immunoblots of TNF-α, and IL-1β in 3-4 months WT and APP/PS1 prefrontal cortex . **(E)** Quantification of TNF-α, and IL-1β protein levels in (D). ($n = 6$ in each group, Student's t-test). All data are presented as mean±SEM. $^{*}p < 0.05$, $^{**}p < 0.01$, $^{***}p < 0.001$.

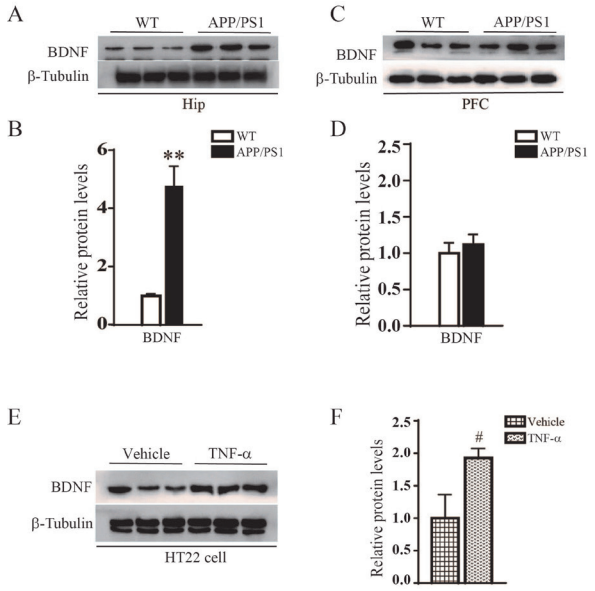


**Figure 4. Increased BDNF level in 3-4 months APP/PS1 hippocampus. (A)** Representative immunoblots of BDNF in 3-4 months WT and APP/PS1 hippocampus. **(B)** Quantification of BDNF protein levels in (A). **(C)** Representative immunoblots of BDNF in 3-4 months WT and APP/PS1 prefrontal cortex. **(D)** Quantification of BDNF protein levels in (C). **(E)** Representative immunoblots of BDNF in HT22 cells treated by TNF-α or vehicle control. **(F)** Quantification of BDNF protein levels in (E). ($n$ = 3 in each group, Student's $t$-test). All data are presented as mean ± SEM. $^{**}p < 0.01$ *vs.* WT; $^{\#}p < 0.05$ *vs.* vehicle control.

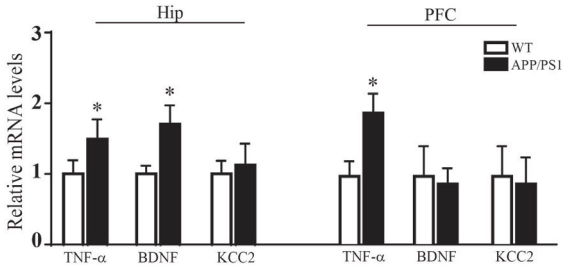


**Figure 6. Increased mRNA levels of TNF-α and BDNF in 3-4 months APP/PS1 hippocampus.** The QPCR results of TNF-α, BDNF and KCC2 mRNA levels in the hippocampus and prefrontal cortex of 3-4 months WT and APP/PS1 mice. ($n$ = 6 in each group, Student's $t$-test). All data are presented as mean ± SEM. $^{*}p < 0.05$.

inflammasomes can promote the production and release of pro-inflammatory cytokines (*31*). We next examined whether increased inflammatory factors level was regulated by activation of inflammasomes. We performed western blotting to detect NLRP-1 and NLRP-3 protein levels in the hippocampus and prefrontal cortex, and found no significant difference between WT and APP/PS1 mice (Figure S1A-D, *http://www.biosciencetrends.com/action/getSupplementalData.php?ID=83*).These results demonstrated that increased soluble Aβ42 level may lead to increased neuroinflammation in 3-4 months APP/PS1 mice, which is much earlier than Aβ plagues formation.

### 3.3. Increased TNF-α levels induced an excess of BDNF level in 3-4 months APP/PS1 hippocampus

TNF-α can up-regulate BDNF protein levels in nerve injury tissues and astrocytes (*17-19*). While excess BDNF can damage neurons. As shown in Figure 4 and Figure 6, we found the protein and mRNA levels of BDNF were both increased in 3-4 months APP/PS1 hippocampus (Figure 4A-D; Figure 6). In addition, we used TNF-α (10 ng/mL) to treat HT22 neuron for 3 h, and found BDNF protein level was significantly increased when treated with TNF-α (Figure 4E-F). These results indicated that BDNF mRNA and protein levels were both increased in 3-4 months APP/PS1 hippocampus, which may be caused by increased neuroinflammation.

### 3.4. KCC2 and $GABA_AR$ levels were decreased in APP/PS1 hippocampus

BDNF-induced TrkB can inhibit $GABA_A$ synaptic responses by down-regulating the KCC2 expression and impairs neuronal $Cl^-$ extrusion (*15,20-22*). By western blotting, we found KCC2 and $GABA_AR$ protein levels were significantly decreased in 3-4 months APP/PS1 hippocampus (Figure 5A-B), while no change in prefrontal cortex (Figure 5C-D). Real-time PCR results showed unchanged KCC2 mRNA level in hippocampus and prefrontal cortex (Figure 6). In contrast, levels of $GABA_BR$, AMPAR, and PSD95 were similar between WT and APP/PS1 mice. (Figure 5A-D; Figure S2A-D, *http://www.biosciencetrends.com/action/getSupplementalData.php?ID=83*). Next we used a selective KCC2 activator, CLP257 (100 μM) to treat HT22 neuron for 2 h, and found a significantly increased KCC2 and $GABA_AR$ protein levels when treated with CLP257 (Figure 5E-F). Furthermore, we also found that KCC2 and $GABA_AR$ protein levels were decreased in 1-2 months APP/PS1 hippocampus (Figure 5G-H). These results demonstrated that inhibitory function were impaired in early APP/PS1 hippocampus. Restore KCC2 can rescue $GABA_AR$ protein level by enhancing chloride extrusion. In order to make sure whether impaired GABA inhibition can lead to abnormal behavior in 3-4 months APP/PS1 mice, we performed open field test, elevated-plus maze, forced swim test, and tail suspension test. The results showed that APP/PS1 mice at 3-4 months not showed anxiety-like and depressive behavior compared to WT controls (Figure S3A-J, *http://www.biosciencetrends.com/action/getSupplementalData.php?ID=83*).

### 3.5. Increased inhibitory protein levels by inhibition of Aβ production

In order to explore whether these changes were caused by increased soluble Aβ42, 3-4 months APP/PS1 mice were treated with LY411575, a potent γ-secretase

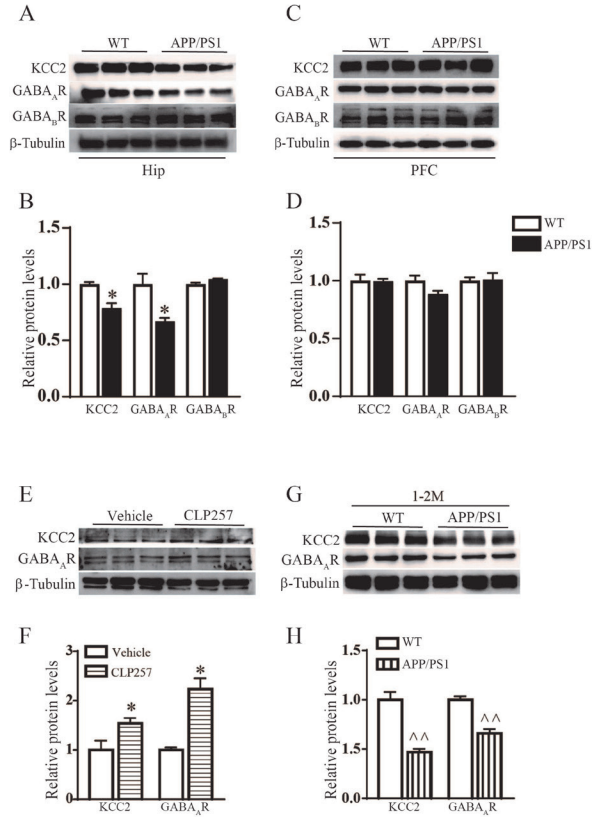


**Figure 5. Decreased inhibitory protein levels in 3-4 months APP/PS1 hippocampus. (A)** Representative immunoblots of KCC2, $GABA_AR$, and $GABA_BR$ in 3-4 months WT and APP/PS1 hippocampus. **(B)** Quantification of KCC2, $GABA_AR$, and $GABA_BR$ protein levels in (A). **(C)** Representative immunoblots of KCC2, $GABA_AR$, and $GABA_BR$ in 3-4 months WT and APP/PS1 prefrontal cortex. **(D)** Quantification of KCC2, $GABA_AR$, and $GABA_BR$ protein levels in (C). **(E)** Representative immunoblots of KCC2 and $GABA_AR$ protein levels in HT22 cell treated by CLP257 or vehicle control. **(F)** Quantification of KCC2 and $GABA_AR$ protein levels in (E). **(G)** Representative immunoblots of KCC2 and $GABA_AR$ in 1-2 months WT and APP/PS1 hippocampus. **(H)** Quantification of KCC2 and $GABA_AR$ protein levels in (G). ($n$ = 6 in each group, Student's $t$-test). All data are presented as mean ± SEM. $^{*}p < 0.05$, $^{**}p < 0.01$ *vs.* 3-4 months WT; $^{\wedge\wedge}p < 0.01$ *vs.* 1-2 months WT.

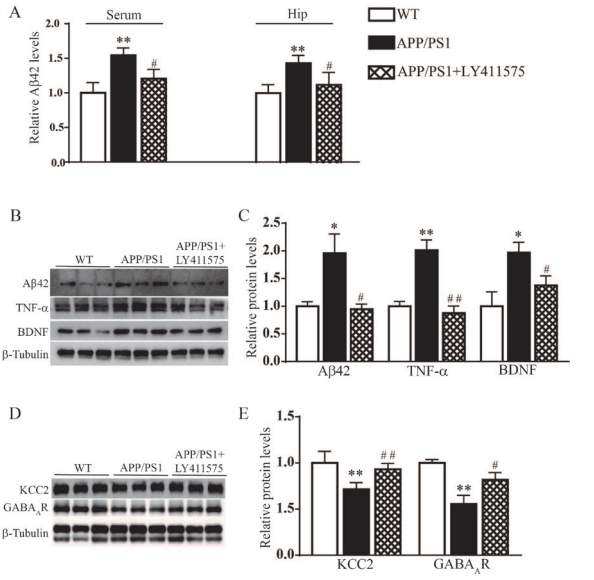


**Figure 7. Reducing interstitial fluid levels of Aβ can reduce BDNF , increase inhibitory protein levels in APP/PS1 hippocampus. (A)** The soluble Aβ42 levels in serum and hippocampus of 3-4 months APP/PS1 mice treated with LY411575 by ELISA. ($n$ = 6 in each group). **(B)** Representative immunoblots of Aβ42, TNF-α, and BDNF. **(C)** Quantification of Aβ42, TNF-α, and BDNF protein levels in (B). **(D)** Representative immunoblots of KCC2 and $GABA_AR$. **(E)** Quantification of KCC2 and $GABA_AR$ protein levels in (D). ($n$ = 3 in each group, one-way ANOVA). All data are presented as mean ± SEM. $^{*}p < 0.05$, $^{**}p < 0.01$ *vs.* WT; $^{\#}p < 0.05$, $^{\#\#}p < 0.01$ *vs.* APP/PS1.

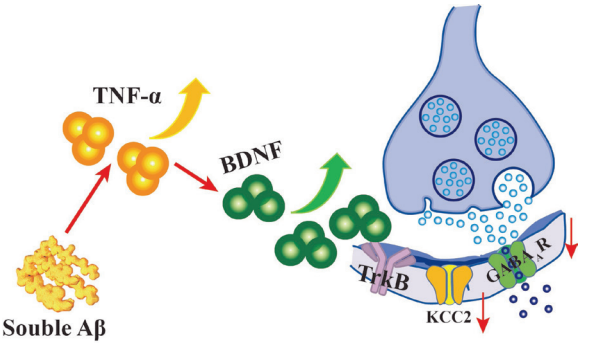


**Figure 8. A working model shows the mechanism underlying soluble Aβ regulation of $GABA_AR$ mediated inhibition in the hippocampus.** The soluble Aβ42 level were elevated in the hippocampus of the early stage of AD mice, which can lead to TNF-α release from astrocyte and microglia. Increased TNF-α up regulated BDNF mRNA and protein levels in hippocampus. Excess BDNF can lead to downregulated KCC2 expression which causes impaired GABA inhibition.

inhibitor by intraperitoneal injection, 2mg/kg/day, for 2 days. ELISA result showed that the soluble Aβ42 was remarkably decreased in serum and hippocampus of 3-4 months APP/PS1 mice when treated with LY411575 (Figure 7A). As shown in Figure 7B-E, western blot result showed that Aβ42, TNF-α, and BDNF protein levels were significantly decreased, while KCC2 and $GABA_AR$ protein levels were increased when treated with LY411575 (Figure 7B-E). These results indicated that soluble Aβ impaired the GABA inhibition most likely by mediating KCC2 level in early APP/PS1 mice.

## 4. Discussion

In this study, we found an impaired GABA inhibition in the early AD mice, which may be caused by increased soluble Aβ42 as summarized in (Figure 8). This conclusion is supported by several lines of evidence: 1) In 3-4 months APP/PS1 mice, soluble Aβ42 was significantly increased without plaque formation. 2) In 3-4 months APP/PS1 hippocampus, TNF-α and BDNF levels were significantly increased, while KCC2 and $GABA_AR$ were decreased. 3) After treated with LY411575, a potent γ-secretase inhibitor, the levels of soluble Aβ42, TNF-α, BDNF, KCC2 and $GABA_AR$ levels can be rescued.

In the last decade, extensive studies indicated that the presence of soluble amyloid-β, an early pathological feature, triggers synaptic dysfunction and cognitive decline in AD (*32-34*). It was reported that the soluble Aβ content of human brain is better correlated with the severity of the disease than are plaques (*35,36*) and biochemically-measured levels of soluble Aβ, including soluble oligomers, correlate much better with the presence and degree of cognitive deficits than do simple plaque counts (*36-38*). Haass, *et al.* (*39*) hypothesized that diffusible oligomers have the principal role, particularly during the earliest, even pre-symptomatic, stages of the AD process. Ample evidence points towards an Aβ-dependent impairment at both inhibitory (*40,41*) and excitatory synapses (*42,43*). The neurotoxic soluble Aβ oligomers, including the most toxic oligomeric Aβ42, have been shown to alter synaptic plasticity and synaptic transmission in various AD animal models *via* a variety of synaptic targets of Aβ (*44*). In our study, we found that soluble Aβ42 level was increased in serum, hippocampus and prefrontal cortex in 3-4 months APP/PS1 mice, which was much earlier than Aβ plaque formation.

Converging lines of evidence support that soluble Aβ are the principal cytotoxic agents that induce a complex array of downstream effects on neurons, microglia, astrocytes and cerebral microvessels in AD (*32*). Neuroinflammation in AD is thought to be primarily driven by microglial cells. Microglial cells continued interactions with soluble and fibrillar Aβ can lead to an inflammatory response resulting in neurotoxicity (*6*). Aβ oligomers and fibrils enhanced the production of inflammatory cytokines and chemokines (interleukin-1, interleukin-6, tumor necrosis factor α (TNF-α), C1q, *etc.*) by priming microglial cells through activated NF-κB and NLRP3 (*6-8*). Primary microglia of rodent and human cultures stimulated with Aβ showed the release of high levels of TNF-α (*9,45*). Numerous studies indicated that TNF-α levels are higher in the cerebrospinal fluid (CSF) of AD patients (*9-11*). TNF-α is a pivotal role in neuroinflammation and a very attractive pharmacological target (*9*). According to a study showed a reduction of TNF-α signaling in rodent models of AD significantly decreased AD-like brain pathology accompanied by an amelioration of cognitive function (*12*). Furthermore, overproduction of TNF-α associated with lower hippocampal volume and with a greater likelihood of mild cognitive impairment (MCI) patient conversion to AD (*12-14*). In our study, we found TNF-α protein and mRNA levels were both increased in hippocampus and prefrontal cortex of APP/PS1 mice. TNF-α capable increased the protein and mRNA expression of BDNF in nerve injury tissues and astrocytes (*17-19*). Astrocytes are one of the sources of BDNF expression and secretion (*17,46*). Our results showed that the BDNF level was increased in 3-4 months APP/PS1 hippocampus. BDNF can protect the nervous system and neuronal plasticity but its excess can cause the opposite effect (*15,16*). BDNF can regulate KCC2 expression by TrkB receptors, which regulated neuronal $Cl^-$ extrusion (*15*). BDNF bound TrkB phosphotyrosine 816 (Y816) by the PLCγ1 pathway inhibits KCC2 mRNA transcription and bound TrkB phosphotyrosine 515 by the Shc pathway promotes KCC2 mRNA transcription (*47*). However, excess BDNF can activate both the PLCγ1 and Shc signaling which leads to KCC2 expression downregulated. KCC2 expression is downregulated following activation of both the PLCγ1 and Shc signaling cascades of the BDNF-TrkB pathway in damaged neurons (*48,49*). In mature neurons, BDNF activates neuronal m-Calpain, which irreversible inactivation of KCC2 *via* MAPK-mediated phosphorylation (*50,51*). We found KCC2 protein level was decreased in APP/PS1 hippocampus. These results demonstrated that increased TNF-α in the hippocampus of early AD mice can stimulate a large amount of BDNF expression and thus suppresses KCC2 expression.

Synaptic failure is an early pathological feature of AD (*52*), including GABAergic activity (*53*). γ-aminobutyric acid (GABA), which a principle inhibitory neurotransmitter in the mammalian central nervous system (CNS)mediates synaptic inhibition by acting on $GABA_A$ and $GABA_B$ receptors ($GABA_AR$, $GABA_BR$) (*22,54*). In the vertebrate brain, $GABA_AR$ mediate the majority of fast inhibition in the brain, and the $GABA_BR$ mediated inhibition is less efficient (*22,23*). $GABA_A$ receptors mediate inhibition depended on the intracellular $Cl^-$ ($[Cl^-]_i$) concentration(*22*). KCC2, which set the proper $[Cl^-]i$ by transporting $Cl^-$ against the concentration gradient is a crucial regulator of GABA-mediated hyperpolarization (*24*). Several previous studies indicated the loss of KCC2 activity orchestrates a depolarizing shift in $E_{GABA}$ which implicated in cortical development systems such as neuro- and synaptogenesis (*25,26*). Previously, we found that restore KCC2 can increase $GABA_AR$ protein level by enhancing $Cl^-$ extrusion (*55*). Our current data shows a decreased $GABA_AR$ protein level in APP/PS1 hippocampus, which may be result of reduced KCC2 level. Several studies showed that exogenous BDNF could decrease presynaptic GABA release and postsynaptic $GABA_AR$ response (*56-58*). When exposure to BDNF, the number of $GABA_A$ receptor rapid reduced in postsynaptic, which is responsible for the decline in GABAergic mIPSC amplitudes (*57,58*). It has been demonstrated that the subunit compositions of $GABA_ARs$ are altered in some regions of the cortex and hippocampus in AD independent of age-related changes (*59,60*). There is accumulating evidence, which indicates that GABAergic neurotransmission also undergoes profound pathological changes in AD (*61,62*) and may be a promising therapeutic target for this neurodegenerative disorder (*63,64*). These results demonstrated that excessive BDNF prevents neuronal $Cl^-$ extrusion by inhibited the expression of KCC2, thereby impaired GABA inhibition.

Taken together, stimulated overproduction of TNF-α

by elevated soluble Aβ42 activated the BNDF-TrkB-KCC2 pathway and thus inhibited $Cl^-$ extrusion, which causes impaired GABA inhibition in early AD mice. These phenotypes were much earlier than Aβ plaque formation. To our knowledge, our present study is the first to report that soluble Aβ42 impaired GABA inhibition *via* mediating KCC2. And our study provides a clue that the role of GABAergic synaptic transmission in the early AD and KCC2 may be a biomarker for the study of early diagnosis of AD.

**Acknowledgements**

The authors greatly thanks for Zhiru Fang from Department of Pharmacology, School of Basic Medical Sciences, Anhui Medical University for technical assistance.

*Funding*: This study was supported by grants from the National Natural Science Foundation of China (No.81801064) and Grants for Scientific Research of BSKY (No. XJ201722) from Anhui Medical University.

*Conflict of Interest*: The authors have no conflicts of interest to disclose.

*Author Contributions:* Ming Chen and Jin-yu Mei conceived, designed and supervised the research project, received funding; Yuan Zhou, Yu-jie Cheng, Yong Li, Ji-yao Ma and Zhi-han Wu performed the research project; Yuan Zhou, Yu-jie Cheng and Yong Li analyzed experimental data, interpreted experimental results; Yuan Zhou drafted the manuscript; Ming Chen reviewed the manuscript. All authors read and approved the final manuscript.

**References**

1. 2019 Alzheimer's disease facts and figures. Alzheimers Dement. 2019; 15:321-387.
2. Daulatzai MA. Early stages of pathogenesis in memory impairment during normal senescence and Alzheimer's disease. J Alzheimers Dis. 2010; 20:355-67.
3. Alber J, Goldfarb D, Thompson LI, Arthur E, Hernandez K, Cheng D, DeBuc DC, Cordeiro F, Provetti-Cunha L, den Haan J, Van Stavern GP, Salloway SP, Sinoff S, Snyder PJ. Developing retinal biomarkers for the earliest stages of Alzheimer's disease: What we know, what we don't, and how to move forward. Alzheimers Dement. 2020; 16:229-243.
4. Chen JX, Yan SS. Role of mitochondrial amyloid-beta in Alzheimer's disease. J Alzheimers Dis. 2010;20 Suppl 2:S569-578.
5. Crews L, Masliah E. Molecular mechanisms of neurodegeneration in Alzheimer's disease. Hum Mol Genet. 2010; 19R1:12-20.
6. Gold M, El Khoury J. beta-amyloid, microglia, and the inflammasome in Alzheimer's disease. Semin Immunopathol. 2015; 37:607-611.
7. Heppner FL, Ransohoff RM, Becher B. Immune attack: the role of inflammation in Alzheimer disease. Nat Rev Neurosci. 2015; 16:358-372.
8. Marttinen M, Takalo M, Natunen T, Wittrahm R, Gabbouj S, Kemppainen S, Leinonen V, Tanila H, Haapasalo A, Hiltunen M. Molecular Mechanisms of Synaptotoxicity and Neuroinflammation in Alzheimer's Disease. Front Neurosci. 2018; 12:963.
9. Decourt B, Lahiri DK, Sabbagh MN. Targeting Tumor Necrosis Factor Alpha for Alzheimer's Disease. Curr Alzheimer Res. 2017; 14:412-25.
10. Zhao M, Cribbs DH, Anderson AJ, Cummings BJ, Su JH, Wasserman AJ, Cotman CW. The induction of the TNFalpha death domain signaling pathway in Alzheimer's disease brain. Neurochem Res. 2003; 28:307-318.
11. Hennessy E, Gormley S, Lopez-Rodriguez AB, Murray C, Murray C, Cunningham C. Systemic TNF-alpha produces acute cognitive dysfunction and exaggerated sickness behavior when superimposed upon progressive neurodegeneration. Brain Behav Immun. 2017; 59:233-244.
12. Sudheimer KD, O'Hara R, Spiegel D, Powers B, Kraemer HC, Neri E, Weiner M, Hardan A, Hallmayer J, Dhabhar FS. Cortisol, cytokines, and hippocampal volume interactions in the elderly. Front Aging Neurosci. 2014; 6:153.
13. Tarkowski E, Andreasen N, Tarkowski A, Blennow K. Intrathecal inflammation precedes development of Alzheimer's disease. J Neurol Neurosurg Psychiatry. 2003; 74:1200-5.
14. Liu Y, Zhou LJ, Wang J, *et al.* TNF-alpha Differentially Regulates Synaptic Plasticity in the Hippocampus and Spinal Cord by Microglia-Dependent Mechanisms after Peripheral Nerve Injury. J Neurosci. 2017; 37:871-881.
15. Lee-Hotta S, Uchiyama Y, Kametaka S. Role of the BDNF-TrkB pathway in KCC2 regulation and rehabilitation following neuronal injury: A mini review. Neurochem Int. 2019; 128:32-38.
16. Ziemlinska E, Kugler S, Schachner M, Wewior I, Czarkowska-Bauch J, Skup M. Overexpression of BDNF increases excitability of the lumbar spinal network and leads to robust early locomotor recovery in completely spinalized rats. PLoS One. 2014; 9:e88833.
17. Saha RN, Liu X, Pahan K. Up-regulation of BDNF in astrocytes by TNF-alpha: a case for the neuroprotective role of cytokine. J Neuroimmune Pharmacol. 2006; 1:212-222.
18. Su WF, Wu F, Jin ZH, Gu Y, Chen YT, Fei Y, Chen H, Wang YX, Xing LY, Zhao YY, Yuan Y, Tang X, Chen G. Overexpression of P2X4 receptor in Schwann cells promotes motor and sensory functional recovery and remyelination *via* BDNF secretion after nerve injury. Glia. 2019; 67:78-90.
19. Bucker J, Fries GR, Kapczinski F, Post RM, Yatham LN, Vianna P, Bogo Chies JA, Gama CS, Magalhaes PV, Aguiar BW, Pfaffenseller B, Kauer-Sant'Anna M. Brain-derived neurotrophic factor and inflammatory markers in school-aged children with early trauma. Acta Psychiatr Scand. 2015; 131:360-368.
20. Rivera C, Li H, Thomas-Crusells J, Lahtinen H, Viitanen T, Nanobashvili A, Kokaia Z, Airaksinen MS, Voipio J, Kaila K, Saarma M. BDNF-induced TrkB activation down-regulates the $K^+$-$Cl^-$cotransporter KCC2 and impairs neuronal $Cl^-$ extrusion. J Cell Biol. 2002; 159:747-752.
21. Tanaka T, Saito H, Matsuki N. Inhibition of $GABA_A$ synaptic responses by brain-derived neurotrophic factor

(BDNF) in rat hippocampus. J Neurosci. 1997; 17:2959-2966.
22. Porcher C, Medina I, Gaiarsa JL. Mechanism of BDNF Modulation in GABAergic Synaptic Transmission in Healthy and Disease Brains. Front Cell Neurosci. 2018; 12:273.
23. Ben-Ari Y, Gaiarsa JL, Tyzio R, Khazipov R. GABA: A pioneer transmitter that excites immature neurons and generates primitive oscillations. Physiol Rev. 2007; 87:1215-1284.
24. Ben-Ari Y. Excitatory actions of gaba during development: the nature of the nurture. Nature Reviews Neuroscience. 2002; 3:728-739.
25. Vanhatalo S, Palva JM, Andersson S, Rivera C, Voipio J, Kaila K. Slow endogenous activity transients and developmental expression of $K^+$-$Cl^-$ cotransporter 2 in the immature human cortex. The European journal of neuroscience. 2005; 22:2799-2804.
26. Rivera C, Voipio J, Payne JA, Ruusuvuori E, Lahtinen H, Lamsa K, Pirvola U, Saarma M, Kaila K. The $K^+/Cl^-$ co-transporter KCC2 renders GABA hyperpolarizing during neuronal maturation. Nature. 1999; 397: 251-255.
27. Molinaro G, Battaglia G, Riozzi B, Di Menna L, Rampello L, Bruno V, Nicoletti F. Memantine treatment reduces the expression of the $K^+/Cl^-$ cotransporter KCC2 in the hippocampus and cerebral cortex, and attenuates behavioural responses mediated by GABA(A) receptor activation in mice. Brain Res. 2009; 1265:75-79.
28. Tang BL. Amyloid Precursor Protein (APP) and GABAergic Neurotransmission. Cells. 2019; 8:550.
29. Najm R, Jones EA, Huang Y. Apolipoprotein E4, inhibitory network dysfunction, and Alzheimer's disease. Mol Neurodegener. 2019; 14:24.
30. Kummer JA, Broekhuizen R, Everett H, Agostini L, Kuijk L, Martinon F, van Bruggen R, Tschopp J. Inflammasome components NALP 1 and 3 show distinct but separate expression profiles in human tissues suggesting a site-specific role in the inflammatory response. J Histochem Cytochem. 2007; 55:443-452.
31. Strowig T, Henao-Mejia J, Elinav E, Flavell R. Inflammasomes in health and disease. Nature. 2012; 481:278-286.
32. Walsh D, Selkoe D. Aβ Oligomers - A decade of discovery. J Neurochem. 2007; 101:1172-1184.
33. Mhillaj E, Morgese MG, Tucci P, Furiano A, Luongo L, Bove M, Maione S, Cuomo V, Schiavone S, Trabace L. Celecoxib Prevents Cognitive Impairment and Neuroinflammation in Soluble Amyloid beta-treated Rats. Neuroscience. 2018; 372:58-73.
34. Selkoe DJ, Hardy J. The amyloid hypothesis of Alzheimer's disease at 25 years. EMBO Mol Med. 2016; 8: 595-608.
35. Roher A, Chaney M, Kuo Y-M, Webster S, Stine W, J. Haverkamp L, Woods A, J. Cotter R, M. Tuohy J, Krafft G, S. Bonnell B, R. Emmerling M. Morphology and Toxicity of A -(1-42) Dimer Derived from Neuritic and Vascular Amyloid Deposits of Alzheimer's Disease. J Biol Chem. 1996; 271:20631-35.
36. Lue LF, Kuo YM, Roher AE, Brachova L, Shen Y, Sue L, Beach T, Kurth JH, Rydel RE, Rogers J. Soluble Amyloid β Peptide Concentration as a Predictor of Synaptic Change in Alzheimer's Disease. Am J Pathol. 1999; 155:853-862.
37. McLean CA, Cherny RA, Fraser FW, Fuller SJ, Smith MJ, Beyreuther K, Bush AI, Masters CL. Soluble pool of Abeta amyloid as a determinant of severity of neurodegeneration in Alzheimer's disease. Ann Neurol. 1999; 46:860-866.
38. Näslund J, Haroutunian V, Mohs R, Davis KL, Davies P, Greengard P, Buxbaum JD. Correlation between elevated levels of amyloid β-peptide in the brain and cognitive decline. JAMA. 2000; 283:1571-7.
39. Haass C, Selkoe DJ. Soluble protein oligomers in neurodegeneration: lessons from the Alzheimer's amyloid beta-peptide. Nat Rev Mol Cell Biol. 2007; 8:101-112.
40. Verret L, O Mann E, B Hang G, M I Barth A, Cobos I, Ho K, Devidze N, Masliah E, Kreitzer A, Mody I, Mucke L, Palop J. Inhibitory Interneuron Deficit Links Altered Network Activity and Cognitive Dysfunction in Alzheimer Model. Cell. 2012; 149:708-721.
41. Palop JJ, Mucke L. Network abnormalities and interneuron dysfunction in Alzheimer disease. Nat Rev Neurosci. 2016; 17:777-792.
42. Lerdkrai C, Asavapanumas N, Brawek B, Kovalchuk Y, Mojtahedi N, Olmedillas Del Moral M, Garaschuk O. Intracellular $Ca^{2+}$ stores control *in vivo* neuronal hyperactivity in a mouse model of Alzheimer's disease. Proc Natl Acad Sci U S A. 2018; 115:E1279-E1288.
43. Zott B, Simon MM, Hong W, Unger F, Chen-Engerer H-J, Frosch MP, Sakmann B, Walsh DM, Konnerth A. A vicious cycle of β amyloid-dependent neuronal hyperactivation. Science. 2019; 365:559-565..
44. He Y, Wei M, Wu Y, Qin H, Li W, Ma X, Cheng J, Ren J, Shen Y, Chen Z, Sun B, Huang FD, Shen Y, Zhou YD. Amyloid β oligomers suppress excitatory transmitter release *via* presynaptic depletion of phosphatidylinositol-4,5-bisphosphate. Nat Commun. 2019; 10:1193.
45. Dhawan G, Floden AM, Combs CK. Amyloid-beta oligomers stimulate microglia through a tyrosine kinase dependent mechanism. Neurobiol Aging. 2012; 33:2247-2261.
46. Ohno Y, Kinboshi M, Shimizu S. Inwardly Rectifying Potassium Channel Kir4.1 as a Novel Modulator of BDNF Expression in Astrocytes. Int J Mol Sci. 2018; 19:3313.
47. Rivera C, Voipio J, Thomas-Crusells J, Li H, Emri Z, Sipila S, Payne JA, Minichiello L, Saarma M, Kaila K. Mechanism of activity-dependent downregulation of the neuron-specific K-Cl cotransporter KCC2. J Neurosci. 2004; 24:4683-4691.
48. Kaila K, Price TJ, Payne JA, Puskarjov M, Voipio J. Cation-chloride cotransporters in neuronal development, plasticity and disease. Nat Rev Neurosci. 2014; 15:637-654.
49. Beggs S, Trang T, Salter MW. P2X4R+ microglia drive neuropathic pain. Nat Neurosci. 2012; 15:1068-1073.
50. Puskarjov M, Ahmad F, Kaila K, Blaesse P. Activity-dependent cleavage of the K-Cl cotransporter KCC2 mediated by calcium-activated protease calpain. J Neurosci. 2012; 32:11356-11364.
51. Zadran S, Jourdi H, Rostamiani K, Qin Q, Bi X, Baudry M. Brain-derived neurotrophic factor and epidermal growth factor activate neuronal m-calpain *via* mitogen-activated protein kinase-dependent phosphorylation. J Neurosci. 2010; 30:1086-1095.
52. Selkoe DJ. Alzheimer's disease is a synaptic failure. Science. 2002; 298:789-791.
53. Verret L, Mann EO, Hang GB, Barth AM, Cobos I, Ho K, Devidze N, Masliah E, Kreitzer AC, Mody I, Mucke L, Palop JJ. Inhibitory interneuron deficit links altered network activity and cognitive dysfunction in Alzheimer model. Cell. 2012; 149:708-721.
54. Succol F, Fiumelli H, Benfenati F, Cancedda L, Barberis A.

Intracellular chloride concentration influences the $GABA_A$ receptor subunit composition. Nat Commun. 2012; 3:738.
55. Chen M, Wang J, Jiang J, Zheng X, Justice NJ, Wang K, Ran X, Li Y, Huo Q, Zhang J, Li H, Lu N, Wang Y, Zheng H, Long C, Yang L. APP modulates KCC2 expression and function in hippocampal GABAergic inhibition. Elife. 2017; 6:e20142.
56. Brady ML, Pilli J, Lorenz-Guertin JM, Das S, Moon CE, Graff N, Jacob TC. Depolarizing, inhibitory GABA type A receptor activity regulates GABAergic synapse plasticity *via* ERK and BDNF signaling. Neuropharmacology. 2018; 128:324-339.
57. Lemtiri-Chlieh F, Levine ES. BDNF evokes release of endogenous cannabinoids at layer 2/3 inhibitory synapses in the neocortex. J Neurophysiol. 2010; 104:1923-1932.
58. Brunig I, Penschuck S, Berninger B, Benson J, Fritschy JM. BDNF reduces miniature inhibitory postsynaptic currents by rapid downregulation of $GABA_A$ receptor surface expression. Eur J Neurosci. 2001; 13:1320-1328.
59. Govindpani K, Calvo-Flores Guzmán B, Vinnakota C, Waldvogel HJ, Faull RL, Kwakowsky A. Towards a Better Understanding of GABAergic Remodeling in Alzheimer's Disease. Int J Mol Sci. 2017; 18:1813.
60. Kwakowsky A, Calvo-Flores Guzmán B, Pandya M, Turner C, Waldvogel HJ, Faull RL. $GABA_A$ receptor subunit expression changes in the human Alzheimer's disease hippocampus, subiculum, entorhinal cortex and superior temporal gyrus. J Neurochem. 2018; 145:374-392.
61. Gueli MC, Taibi G. Alzheimer's disease: amino acid levels and brain metabolic status. Neurological Sciences. 2013; 34: 1575-79.
62. Ramos-Miguel A, Hercher C, Beasley CL, Barr AM, Bayer TA, Falkai P, Leurgans SE, Schneider JA, Bennett DA, Honer WG. Loss of Munc18-1 long splice variant in GABAergic terminals is associated with cognitive decline and increased risk of dementia in a community sample. Molecular Neurodegeneration. 2015; 10: 65.
63. Vellas B, Sol O, Snyder P, Ousset PJ, Haddad R, Maurin M, Lemarie J-C, Desire L, P Pando M. EHT0202 in Alzheimers Disease: A 3-Month, Randomized, Placebo-Controlled, Double-Blind Study. Curr Alzheimer Res. 2011; 8:203-212.
64. Guerrini G, Ciciani G, Costanzo A, Daniele S, Martini C, Ghelardini C, Di Cesare Mannelli L, Ciattini S. Synthesis of novel cognition enhancers with pyrazolo[5,1-c][1,2,4] benzotriazine core acting at γ-aminobutyric acid type A ($GABA_A$) receptor. Bioorg Med Chem. 2013; 21:2186-2198.

Received June 18, 2021; Revised August 2, 2021; Accepted September 7, 2021.

[§]These authors contributed equally to this work.

**Address correspondence to:*
Ming Chen, Department of Pharmacology, School of Basic Medical Sciences, Anhui Medical University, No.81 Meishan Road, Hefei, Anhui 230032, China.
E-mail: chenming@ahmu.edu.cn

Jinyu Mei, Department of Otorhinolaryngology Head and Neck Surgery, the Second Affiliated Hospital of Anhui Medical University, 678 Furong Road, Hefei, Anhui 230601, China.
E-mail: meijinyu@ahmu.edu.cn

Released online in J-STAGE as advance publication September 16, 2021.